Tuomikoski, S., Virkkala, N., Rovio, S., Hokkanen, A., Sirén, H., Franssila, S., Design and fabrication of integrated solid-phase extraction-zone electrophoresis microchip, Journal of Chromatography A, 1111, (2006), 258-266.

Available online at www.sciencedirect.com
SCIENCE DIRECT
Journal of Chromatography A, 1111 (2006) 258–266
JOURNAL OF CHROMATOGRAPHY A
www.elsevier.com/locate/chroma

Design and fabrication of integrated solid-phase extraction-zone electrophoresis microchip

Santeri Tuomikoski [a,*], Nina Virkkala [a], Stella Rovio [b], Ari Hokkanen [c], Heli Sirén [b], Sami Franssila [a]

[a] *Helsinki University of Technology, Microelectronics Centre, P.O. Box 3500, 02015 Espoo, Finland*
[b] *Technical Research Centre of Finland, VTT Processes, P.O. Box 1600, 02044 Espoo, Finland*
[c] *Technical Research Centre of Finland, VTT Information Technology, P.O. Box 1200, 02044 Espoo, Finland*

Available online 28 October 2005

Abstract

Integrated solid-phase extraction-zone electrophoresis (SPE-ZE) device has been designed and fabricated on microchip. The structures were fabricated by using multiple layers of SU-8 polymer with a novel technique that enables easy alignment and high yield of the chips. SU-8 adhesive bonding has two major advantages: it enables bonding of high aspect ratio pillars and it results in fully SU-8 microchannels with uniform electrokinetic flow properties. The SPE-ZE device has a fluidic reservoir with 15:1 high aspect ratio pillars for bead filters that act as a SPE part in the chip structure. The separation unit is a 25 mm long electrophoresis channel starting from the outlet of SPE reservoir. Argon laser-induced fluorescence (LIF) detector was used to monitor simultaneously the SPE reservoir and the detection site at the end of the electrophoresis channel. Flow characteristics and electric field distributions were simulated with Femlab software. Fluorescein was used as the analyte for detecting the operational performance of the chip. Adsorption, bead rinsing, elution and detection were tested to verify functioning of the chip design.

Keywords: Solid phase extraction; Electrophoresis; Microchip; SU-8; Microchannel

1. Introduction

Development of miniaturized analysis systems has been rapid since late 1990s. Concept of micro total analysis systems (μ-TAS) gives superior features in the field of analysis systems: separation times are shorter and sample and analyte consumption have been reduced significantly in comparison with macroscale equipment. For example, separation times in the range of milliseconds have been demonstrated in microscale devices [1]. However, miniaturized analysis tools do not give desired results, if the sample is very dilute because the total amount of analyte in the separation device remains under detection limit. In that case sample concentration prior to analysis is needed.

Conventional way to clean the samples for microseparation is to use off-line SPE treatment and to analyze the eluate with channel electrophoresis [2]. Lately solid-phase extraction (SPE) has been adapted in the field of microscale separation techniques. In most of the applications described in the literature, SPE is realized by extension of macroscale world to microfluidics. This is done by coating or packing standard capillaries with the SPE matrix. These techniques have been reviewed by Saito and Jinno [3,4]. However, this connection scheme has large dead-volumes. With microfabrication techniques dead volumes can be effectively avoided.

Guzman described an electrophoresis apparatus which contains series of solid phase micro-extraction devices for selective and non-selective molecular consolidation. The devices are used on-line with capillary tubes. The extraction procedure enhances loadability of the analytes, gives better detectability and fastens the throughput of samples. However, no real applications were shown to clarify its performance [5].

Kutter et al. used C18-coated channels in a microfabricated device to demonstrate on-chip solid phase extraction procedure. They obtained 80-fold enrichment concentrations for a neutral dye [6]. For biological purposes Wolfe et al. demonstrated the use of silica-based solid phase extraction system which was used for DNA sequencing. In the system silica beads were packed into the channel using sol-gel network. Nanograms of DNA could be extracted and detected in less than 25 min [7].

A large number of miniaturized approaches to SPE have been done by application of micro-sized beads in microfabricated

* Corresponding author.

0021-9673/$ – see front matter © 2005 Elsevier B.V. All rights reserved.
doi:10.1016/j.chroma.2005.10.021

analysis systems. Beads and SPE sorbents increase surface to volume ratio easily in microfabricated devices giving advances in separations and still have the benefits of microfabrication techniques. Beads can be used also to introduce for example biomolecules to ready-made chips. This is advantageous if desired molecules do not tolerate the conditions of chip fabrication. Few reviews of bead applications in microfabricated devices have been published [8,9]. The most important steps in the bead application are directing the beads to desired places and holding them there. Beads have been stopped in microchips with magnets [10], with ultrasound [11], flow profile [12] or with chemical treatments [13]. However, the easiest integrated method from fabrication point of view is to use mechanical barriers that hinder the flow of beads [14,15]. The bead filters can consist of dam-structure (horizontal barrier) [15] or pillars (vertical structures) [14]. Dam-type structure is simple to fabricate, but it limits the flow of liquid dramatically, and flow profiles are directed non-uniformly resulting in dead volumes on the chip. Pillar-type bead filter allows the flow of liquid more uniformly through the beads. Flow resistance is clearly smaller in pillar-type bead chamber [9].

Microfabrication of pillar-type bead reservoirs for SPE is difficult as comparison to dam-type. Pillars require application of deep reactive ion etching (DRIE) if applying glass or silicon substrates. Etching process for silicon has been well established, but application of high voltages on patterned silicon substrates requires long oxidation processes of weeks [16]. Polymers and glass can provide adequate insulation for high voltage, but these techniques are limited in fabrication of various geometries. DRIE of glass substrates has been limited in depth: maximum values are about 50 μm [17]. Widely applied replication techniques in polymer microfabrication, like casting, hot embossing and injection molding, are suitable for fabrication of large areas with desired depth. However, fabrication of high aspect ratio pillars with these techniques is limited. Lithographic patterning of epoxy photoresist SU-8 provides an easy approach both to high aspect ratio pillar and to multilayer microchannel fabrication.

SU-8 is negative photoresist developed by IBM [18]. Initially, it was applied as standard thick photoresist in applications: as an etching mask or in electroplating [19,20]. Soon its unique properties were appreciated and thereafter SU-8 has been used also as structural material in various components. It is mechanically strong and optically transparent for wavelengths above 350 nm [19]. These properties enable patterning of thick layers with high aspect ratios. Thicknesses over 2 mm and aspect ratios up to 66:1 have been demonstrated with UV exposure of SU-8 [21,22].

Due to mechanical strength of SU-8 it has been used in the field of MEMS and lately it has become increasingly applied in microfluidics [23–26]. The main usage of SU-8 in microfluidics has been application as a master for casting microfluidic channels in polydimethylsiloxane (PDMS) [25,26]. This process has been well established and widely applied due to its simplicity. However, PDMS is suitable for simple structures only, and its limited chemical stability towards solvents prohibits its application in many areas. Microchannels can be easily fabricated to SU-8 itself. Various microchannel geometries can be easily patterned to SU-8 by simple UV-lithography. The main difficulty has been in fabrication of enclosed microchannels. One option is to cover the microchannels by lamination with sheet of different material [27]. However, this affects to the fluidic properties of the channels.

Many approaches for fabrication of fully SU-8 microchannels have been described in the literature including: development of the channel after curing of the roof SU-8 [28], lamination with SU-8 [29] and adhesive bonding [23]. These methods have been performed only for small-scale microfluidic components or the methods are not optimized for fabrication with high yield. This has limited application of SU-8 in the microfluidic components. We have developed lately bonding method for high yielding large area bonding for microfluidic chips [30]. Earlier we have presented adhesive bonding of high aspect ratio SU-8 pillars of simple test structures [31]. We now demonstrate large area bonding of microfluidic devices together with successful bonding of small pillars.

In this study, we have designed and realized an integrated solid-phase extraction-zone electrophoresis (SPE-ZE) device. The microchip was designed and its performance was simulated with Femlab software. This novel integrated microchip was fabricated fully from SU-8. Fabrication process was optimized to give high yield of large area chips. Chip consists of SPE channel with reservoir guarded by pillar-type bead filters to immobilize the solid-phase material. Electrophoresis channel goes perpendicularly to the SPE channel forming cross-shaped fluidic channels. This channel was designed for zone electrophoresis on a microchip. Fluidic testing of the chips was performed with fluorescein samples. Detection was performed with laser-induced fluorescence (LIF) through the cover plate of the chip system.

2. Methods

2.1. Materials and chemicals

Negative photoresists SU-8 50 and SU-8 100 were products of Microchem (Newton, MA, USA) and they were purchased from Micro Resist Technologies (Berlin, Germany). Developer for SU-8 was mr-Dev 600 from Micro Resist Technologies. Chemicals for RCA solutions were hydrogen chloride, hydrogen peroxide, ammonium hydroxide and hydrofluoric acid all from Merck (Darmstadt, Germany). Buffered hydrofluoric acid was SiO-etch 17/02 from Merck.

Sodium salt of fluorescein was a gift from the Laboratory of Analytical Chemistry (University of Helsinki, Finland). Acetic acid and sodium hydroxide (Titrisol) were from Merck. 3-(Cyclohexylamino)-1-propanesulfonic acid (CAPS) was obtained from Sigma (Sigma–Aldrich Chemie, Steinheim, Germany). Ethanol (99.5%) was purchased from Primalco (Rajamäki, Finland). All reagents were of analytical grade. The deionized water was produced with a Milli-Q gradient A10 system (Millipore, Bedford, MA, USA).

2.2. Solutions

Sample introduction solvent 10 mM glacial acetic acid was made by diluting it with Milli-Q water. One hundred and twenty micromolar CAPS was used as the separation buffer. It was made of 200 mM CAPS and 0.1 M sodium hydroxide in 3:2 (v/v). In SPE, the elution solvent was 500 mM CAPS (pH 10.4 adjusted with 0.1 M sodium hydroxide) containing ethanol (40:60, v/v). The separation electrolyte and elution solvent were filtered using GHP Acrodisc syringe filters with 0.45 μm GHP membranes (Pall Gelman Lab., Ann Arbor, MI, USA). Stock solution of fluorescein of 1 mg/ml was prepared in water. The working solutions were diluted from the stock solution with 10 mM acetic acid (pH 3.4).

2.3. Geometry of the chips

Microchip geometry consists of an SPE part and an electrophoresis part as shown schematically in Fig. 1a. In Fig. 1b is shown a corresponding picture of the ready-made microchip. The SPE part is a round reservoir with a diameter of 2 mm and a height of 400 μm. The chip has four fluidic ports that have been numbered 1–4 in Fig. 1a. Fluidic ports 1 and 2 work as inlets and 3 and 4 as outlets of the chip. Port 1 is for introducing the beads to the reservoir. This inlet is completely open to the SPE part of the chip. All three other openings to the reservoir are guarded with high aspect ratio pillars. These pillars are required to keep the extraction medium at the reservoir. Ports 2 and 3 are identical inlet and outlet channels at the sides of reservoir allowing solvent flow through the extraction medium by pressure. Port 4 is an outlet of electrophoresis part of the chip. It starts from the SPE reservoir and is as well guarded by SU-8 pillars. Electrophoresis part is microchannel with cross-section of 50 μm × 50 μm. Analyte is moved in this ZE channel by voltage and pressure.

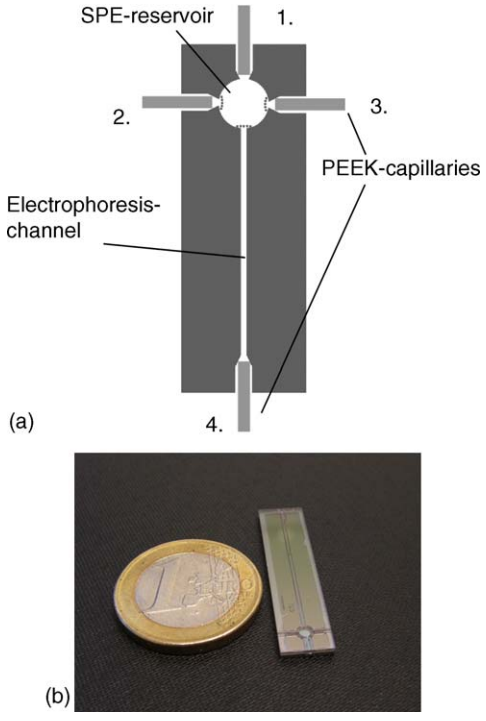

Fig. 1. (a) A Schematic picture of the chip design. Inlets have been numbered for simplicity. (b) Picture of ready SPE-ZE microchip. All the structures are made of SU-8 and glass and silicon wafers are used as a support. A euro coin is used to compare chip size.

2.4. Fabrication of microchips

Microchips were fabricated with three-layer SU-8 process. Structures consisted of two layers of fluidic structures and of one non-patterned SU-8 layer. SU-8 structures were stacked between oxidized silicon wafer and Pyrex wafer. All the wafers applied in the process were 100 mm in diameter. Silicon wafers were from Okmetic (Espoo, Finland). Their orientation was ⟨100⟩ and thickness 525 ± 25 μm. Pyrex wafers were 7740 wafers from Corning (NY, USA).

Silicon wafers were RCA-cleaned by the standard three-solution process. After the initial cleaning, wafers were thermally oxidized. Oxide thickness was 1000 nm. Silicon dioxide was applied to protect from voltage breakthrough via silicon substrate. The SPE reservoir and outlet of electrophoresis channel are open to the silicon oxide in the design of microchip. The electrophoresis channel is fully made of SU-8 and therefore adequately insulated. SU-8 was applied directly on top of silicon oxide without additional chemical treatments. However, dehydration bake at 120 °C was done immediately prior to SU-8 application. Wafers were held in the oven for 90 min.

The processing steps for SU-8 patterning are shown in Fig. 2. SU-8 was applied on wafers statically and spread to the wafer by spinning. The spinning speed and viscosity of applied SU-8 defined the thickness of the layers. Applied process parameters for SU-8 processing are shown in Table 1. Thickness of the first SU-8 layer was adjusted to 350 μm. Baking was done according to basic processing conditions for SU-8 by two step baking first at 65 °C and then at the 95 °C. Slow cooling down to room tem-

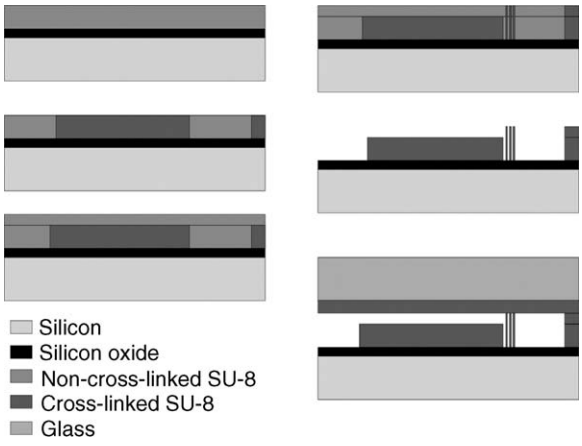

Fig. 2. Process flow for fabrication of SPE-ZE chips. First layer of SU-8 is applied on top of an oxidized silicon wafer. Reservoirs and channels for connection capillaries are patterned to it. Second layer is applied without development in-between. Pillars for bead stopping and ZE channel are patterned in the second exposure. Structures in first two layers are developed at the same time. The third layer of SU-8 is spinned on top of Pyrex wafer and channels are enclosed with adhesive bonding technique.

Table 1
Process parameters for fabrication of SU-8 structures

	Resist	Spinning speed (rpm)	Softbake at 65 °C (min)	Softbake at 95 °C (min)	Exposure dose (mJ/cm^2)	Post exposure bake at 95 °C (min)
Layer 1	SU-8 100	1000	30	120	1875	25
Layer 2	SU-8 50	2500	10	20	3875	55
Layer 3	SU-8 50	2000	15	10	1000	5

perature was required to control and minimize stresses in SU-8 layers. SU-8 baking was done on a contact hotplate. Exposure was done with LOMO EM-5006 mask aligner with broad-band UV illumination. Exposure dose values in the Table 1 are measured at the wavelength of 365 nm. Post exposure bake was done with hotplate ramping temperature to 95 °C during 5 min and then keeping the temperature fixed for the time defined in Table 1. First layer formed the inlets and outlets for the polyether ether ketone (PEEK) capillaries as well as the reservoirs for the beads.

Second layer of SU-8 was applied on top of the first one without development in-between. Second layer forms 50 μm thick electrophoresis channel, pillars for bead stopping and additional 50 μm thickness for all underlying structures. Bead filter pillars were exposed completely at second exposure. It was done through both SU-8 layers forming high aspect ratio pillars with height of the both layers (400 μm). This technique enables fabrication of pillars without alignment problems. The design values for the pillar diameter were 30 μm and 25 μm for the spacing between the pillars. The electrophoresis channel walls were correspondingly formed during the second exposure. Width of the electrophoresis channel was 50 μm.

The roof for the microchannels was done by adhesive bonding with SU-8. Pyrex wafers were initially cleaned by short etching in buffered hydrofluoric acid. Dehydration bake was done similarly as with silicon wafers. Third layer of SU-8 was spinned on top of Pyrex wafer and a short soft bake was done for SU-8. Wafers were cooled from the soft bake temperature and stabilized to 68 °C. After that the wafers were pressed to full contact and allowed to cool to room temperature. Flood exposure was performed through Pyrex wafer and finalizing post exposure bake was performed according to Table 1.

After microfabrication steps SPE-ZE chips were cut by wafer dicing saw (Loadpoint Microace 3) to individual chips. This process also opened the fluidic ports at the sides of the chip. Chips were washed with 2-propanol to remove silicon dust from sawing. Chips were dried from outside by blowing with nitrogen and microchannels were dried with vacuum pump. PEEK capillaries (150 μm I.D. × 360 μm O.D., Upchurch Scientific, Oak Harbor, WA, USA) were inserted from the sides of the chip and the fluidic connections were glued with epoxy adhesive (Araldite Rapid or Araldite 90 Seconds, Bostik, Tampere, Finland). Lithographically defined designs of the fluidic ports prevented capillary penetration into the reservoirs. These can be seen from schematic picture (Fig. 1a). Chip was placed into laboratory made wafer holder (P. Vastamäki, VTT Processes, Espoo, Finland) for the measurements.

2.5. Instrumentation

A peristaltic pump with three fluid transfer channels was used for liquid feeding (model IPC, Ismatec, Glattbrugg, Switzerland). The injection valve was from Rheodyne model 7000L with 2.5 μl sample loop (Rheodyne, Rohnert Park, CA, USA). Four shut-off valves (model P-782, Upchurch Scientific) were used to control fluid movements in chip during the measurements. A high-voltage power supply was from Bertan (Hicksville, NY, USA). Stainless steel tubes of 0.5 mm I.D. × 1/16 in. O.D. were used to apply the high voltage to the separation channel on the chip. The stainless steel tubes were inserted into the separation inlet and outlet liquid junctions approximately 5 cm from chip inlet and 6 cm from chip outlet.

The setup for the laser-induced fluorescence measurement is shown in Fig. 3. The excitation light source was an argon laser (Laser Graphics, 161 LGS, 40 mW). The excitation light was filtered with a 488 ± 5 nm bandpass filter. The chip was arranged in an upright position so that the laser beam had to pass through the cover plate of the microchip. Laser beam was divided to two part with beam splitter. The angle of incidence for the laser beams was about 45°. First laser beam was focused to a 100 μm spot onto the separation channel of the microchip. Second laser beam was guided to SPE reservoir without focusing lens. The fluorescence light was filtered with two 520 ± 5 nm bandpass filters and measured with a CCD camera (Hamamatsu Orca ER, Hamamatsu City, Japan). Second laser beam was attenuated with bandpass filter 488 ± 1 nm so that fluorescence signals of SPE reservoir and separation channel were in the same level. This makes it possible to measure both signals parallel with the CCD camera. Fluorescence measurement window in the separation channel and SPE reservoir was 50 μm × 50 μm and

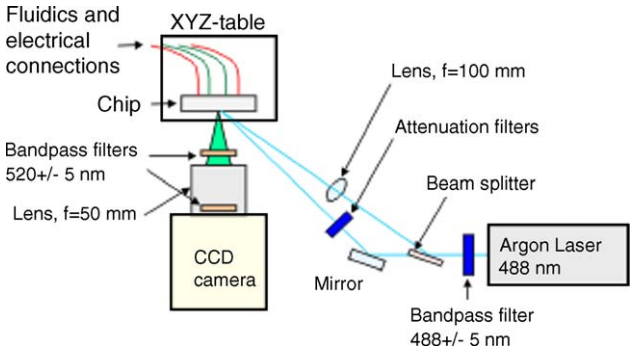

Fig. 3. The fluorescence measurement setup used for the SU-8 microchip. In the setup, there was XYZ table for moving the chip and CCD camera for the detection of signals. LIF was monitoring both the SPE reservoir and the separation channel simultaneously. Detection site in the separation channel was 24 mm from the SPE reservoir.

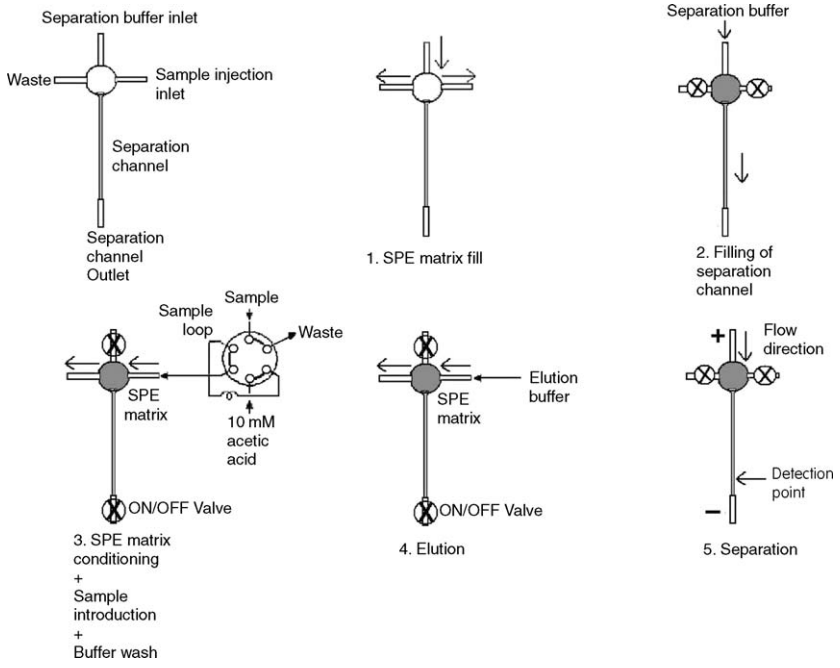

Fig. 4. The chip filling and testing procedures. Horizontal and vertical arrows around the SPE part show the solvent flow directions during the different steps.

1 mm × 1 mm, respectively. The exposure time of the CCD camera was 5 ms.

2.6. Measurements

The SPE reservoir was filled manually with Isolute ENV+SPE matrix (Argonaut Technologies, Hengoed, UK) which is hyper cross-linked hydroxylated polystyrene-divinylbenzene copolymer. The irregular shaped particles have an average size of 90 μm.

The chips were conditioned by rinsing them manually with 0.1 M sodium hydroxide and Milli-Q water prior to use. Solid phase extraction and separation consisted of five step: conditioning of the SPE matrix, sample loading, buffer wash, elution of analyte and separation (Fig. 4). The separation channel was first filled with 120 mM CAPS by pumping of buffer at speed of 13.7 μl/min with simultaneous sequence of 5 s pump on, 5 s pump off. During this stage the sample injection inlet and waste outlet were closed.

After 5 min pumping of separation buffer, the sample analysis was started. The separation channel inlet and outlet were closed and the sample injection inlet and the waste line were opened. The pumping of sample introduction solvent was started at speed of 13.7 μl/min. The sample was injected to the 2.5 μl sample loop, and the valve of sample injector was turned from load to inject position. The flow of the sample introduction solvent, 10 mM acetic acid, conditioned the SPE matrix and carried the sample onto the SPE matrix. The uncharged analyte was retained in the SPE matrix. After the sample loading, the SPE matrix was washed with 10 mM acetic acid. The equilibration, sample loading and buffer wash were carried out in 10 min.

Prior to analyte elution, fluorescence detection was started. The laser beam was divided into two beams, which made it possible to detect the SPE reservoir and the separation channel at the same time. After the sample loading, there was not an increase in signal in SPE reservoir, because the fluorescein did not emit fluorescence at acidic pH. The pumping of elution buffer 500 mM CAPS (pH 10.4)–ethanol (40:60, v/v) was started at speed of 8.8 μl/min. The arrival of the elution buffer to the SPE material could be observed as an increase in signal, because 10 mM acetic acid in the SPE reservoir was replaced with basic elution buffer and fluorescein started to emit fluoresce. When the signal in SPE reservoir reached a plateau or overload point, the pumping of elution buffer was stopped. During elution the separation inlet and outlet were kept closed to prevent sample going to wrong direction.

Immediately after the elution step, separation was started. The elution buffer inlet and waste line were closed and the separation channel inlet and outlet were opened. The pumping of separation buffer with speed of 13.7 μl/min was started at the same time as the high voltage of 4 kV was turned on. The polarity was from anode to cathode. After every separation the SPE matrix was washed with elution buffer 3 min at speed of 10.2 μl/min followed by pumping of separation buffer to the channel.

3. Results and discussion

3.1. Simulation

Fluid flow and electrical field in SPE-ZE device was modeled separately with Femlab program. Modeling was done with physical parameters of water (density 1000 kg/m^3, viscosity 1040×10^{-6} Ns/m^2, permittivity $81 \times 8.85419 \times 10^{-12}$ F/m). Fluid flow model uses incompressible stationary Navier–Stokes equation for finite element method (FEM) calculations. Fluid input is from the left side of reservoir and out is in the right

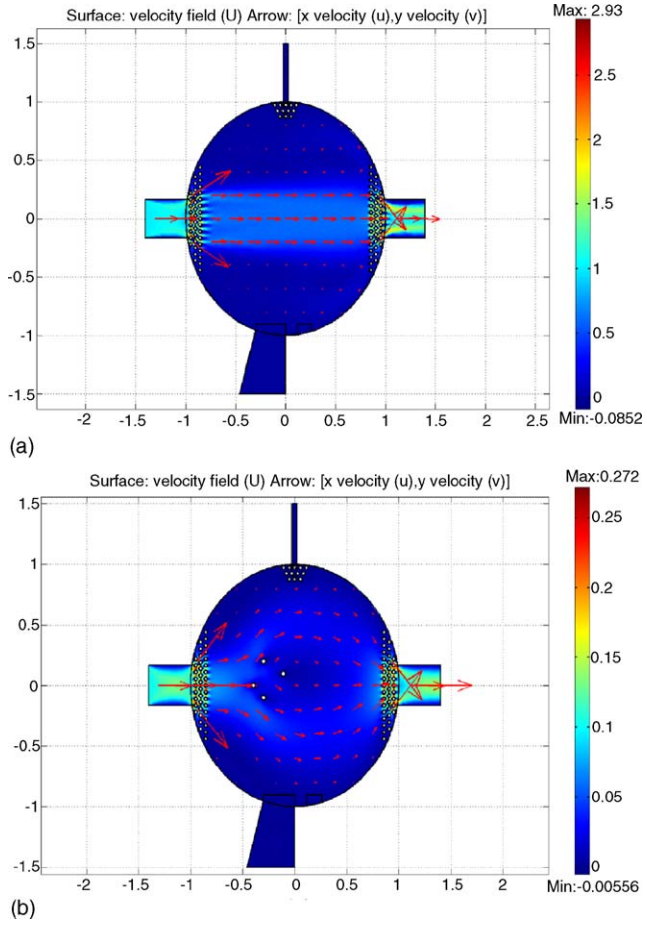

Fig. 5. (a) Simulated fluid flow in SPE reservoir without beads. (b) Simulated fluid flow in the reservoir with beads.

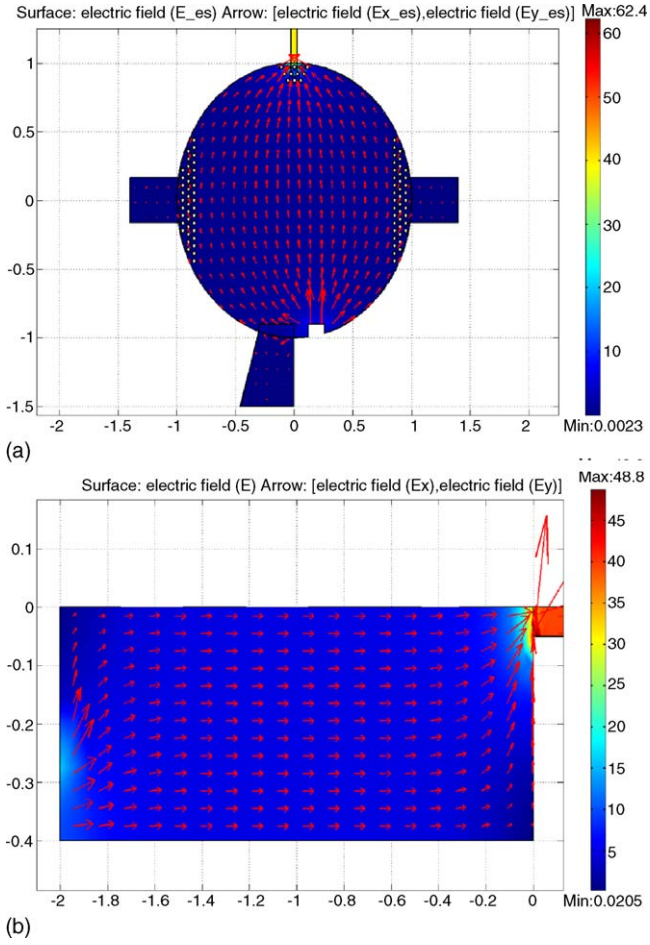

Fig. 6. (a) Electrical field in the chip surface level. (b) Electrical field in the cross section of SPE reservoir.

(Fig. 5). Boundary conditions for input flow velocity were 1 mm/s and output flow has no external pressure. Boundary conditions of other surfaces are no-slip (flow zero). SPE reservoir has 30 μm pillars with 25 μm spacing on both sides. Pillars spread the fluid flow wider (Fig. 5a). Fluid flow in the middle of the reservoir is the highest, but there is also small flow velocity at the edges. Effect of beads was modeled with few individual beads in the SPE reservoir. Completely filled SPE bead reservoir was not used in the model, because of computing power limitations of a desktop computer. Fig. 5b shows velocity field of water with four randomly placed 40 μm beads (input flow velocity 1 mm/s). Stationary beads have strong effect for velocity field. From these results it can be expected that completely filled SPE reservoir has wider fluid flow than an empty SPE reservoir.

Electrical field was modeled in the chip surface level (Fig. 6a) and in the cross-section of SPE reservoir (Fig. 6b). Electric field models use stationary electrostatic equation for FEM calculations. This electric field modeling was done also without beads because the complex geometry of reservoir filled with beads. Electrode of electric field is in the bottom of SPE reservoir (Fig. 6a). Boundary condition for the separation voltage was 2 kV. Ground electrode is in the outlet of electrophoresis channel (out of the picture). Boundary conditions for other surfaces are zero (surface charge). Electric field is highest in the middle of SPE reservoir, but still the whole reservoir has effect for sample during ZE separation. Cross-section model uses the same electrostatic equation for calculations. Boundary conditions are also similar to those in surface level model. Electric field electrode (2 kV) is now at bottom left of the reservoir (Fig. 6b) and the ground electrode is again in the outlet of electrophoresis channel (out of the picture). Other surfaces have zero surface charges. Electrical field spreads in the whole reservoir. The weakest parts of electric field in the reservoir cross-section (Fig. 6b) are up in the left corner and down in the right corner.

3.2. Microfabrication

Two versions of the microchip with different dimensions were realized. The main difference between them was their outer dimensions that were mainly limited by the electrophoresis channel length. The larger one was 6 mm × 60 mm and the smaller one was 8 mm × 32 mm with corresponding electrophoresis channel lengths of 50 mm and 25 mm. Both microchip designs were successfully fabricated and applied in fluidic tests. All the fluidic tests shown in this paper utilize 25 mm long separation channels. Picture of ready-made chip is shown in Fig. 1b. The SU-8 processing was challenging because

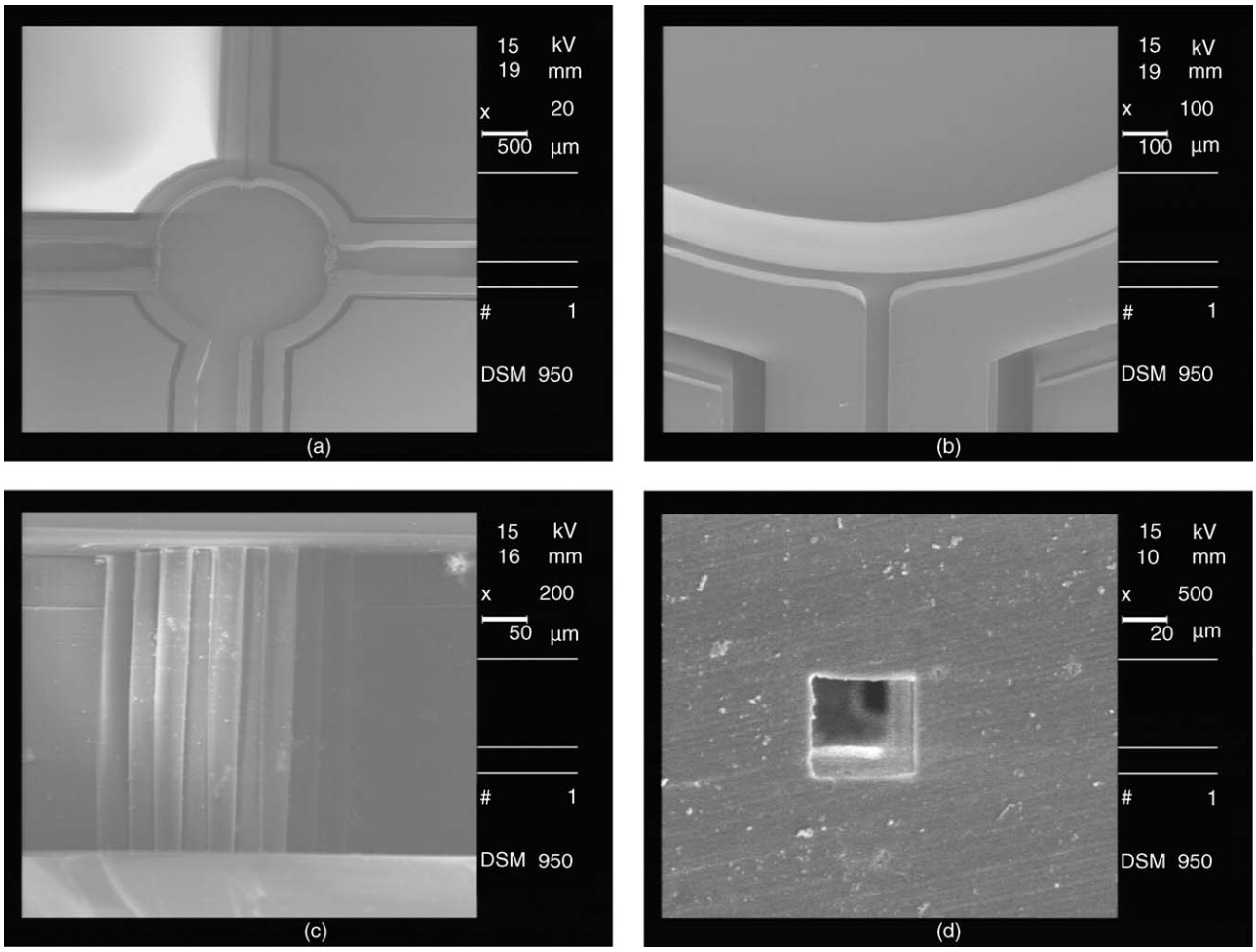

Fig. 7. Scanning electron microscope pictures of the microchip. (a) SPE reservoir before bonding. Top and side channels have high aspect ratio pillar filters. (b) The electrophoresis channel end showing multilayer SU-8 structure. (c) High aspect ratio SU-8 pillars fabricated by single exposure. Successful bonding of the pillars can be seen from the picture. The electrophoresis channel begins behind the pillars. (d) Cross-section of 50 μm × 50 μm electrophoresis channel.

laterally different geometries were produced in relatively thick multilayer SU-8 structure. Fabrication process was developed and optimized to achieve high yield of functioning chips from the wafers.

A number of critical issues were identified in chip processing that limited the yield of functioning chips. Bending or cracking of high aspect ratio SU-8 pillars during processing is major source of erratic chips. This was critical because lack of few pillars removes completely the capability of bead stopping. Bending of the pillars occurs due to stresses in the SU-8 layers. Stresses also complicate alignment and bonding processes. Stresses arise during the baking steps in the fabrication. Slow cooling rates were applied to minimize effect of stress. Despite this residual stresses remain in SU-8 layers and therefore novel fabrication process was required to overcome alignment problem.

Stresses are caused by coefficient of thermal expansion (CTE) difference between SU-8 and supporting wafers. SU-8 has coefficient of thermal expansion (CTE) 52 ppm/°C [32] compared to silicon and Pyrex wafers that have the CTEs around 3 ppm/°C. Effect of CTE difference can be seen with bare eye as bowing of the wafers. Bowing and correspondingly relaxation of bowing over time make alignment of overlapping layers difficult. Alignment with the accuracy required for high aspect ratio pillars was impossible. Therefore pillars were fully patterned in second exposure only eliminating alignment errors. Alignment of overlapping layers was done only for structures that have dimensions in the range of 200 μm. Accuracy of this level was easily achieved. Also bending of the pillars was controlled by the single exposure technique. Picture of non-bonded bead reservoir is shown in Fig. 7a. In Fig. 7b is shown the outlet of the electrophoresis channel. The picture is showing the different levels of SU-8 structures and the alignment error due to stresses in SU-8 layers.

Another major source of problems was the bonding process. Bonding was performed according to our earlier studies [30]. With the application of auxiliary moats in the mask design, good bonding yield was achieved. Auxiliary moats next to the main channel balance stresses in the wafers and allows compensation of thickness non-uniformities in the processed SU-8 layers. However, few chips failed due to blocking of the electrophoresis channel with SU-8 from the bonding layer. Excluding bonding failures yield of functioning chips was 90%. Incidental failures were also due to errors in other processing steps like in chip

sawing. Despite numerous possible failure mechanisms in chip processing, high average yield of 75% of successful chips from the wafers was obtained. This value was calculated from six wafers fabricated with optimized fabrication process.

Bonding of high aspect ratio pillars was successful in these complicated fluidic chips. The results were uniform with those we earlier reported for bonding of high aspect ratio structures in simple test chips [31]. No deformations occurred in pillars during bonding and those were mechanically strong enough for measurements with pressure driven flow. Pressure was applied in these tests manually with syringe applying high force. Bonded pillars from the structures are shown in Fig. 7c. In Fig. 7d is shown cross-section of enclosed electrophoresis channel. Oxide thickness of 1000 nm was enough to protect from breakthrough via silicon substrate.

The fabrication process was relatively simple and straightforward after optimization. SU-8 enables fabrication of fluidic structures with various lateral geometries and correspondingly thickness can be adjusted over wide range. Thickness can be easily up to 1 mm and for lateral dimensions there are no limits for the size. Pillar sizes have to be adjusted for the thickness so that aspect ratio does not increase above 15:1 that can be reproducibly fabricated with SU-8. This enables fabrication of SPE unit for any desired capacity. High aspect ratio pillars can be easily patterned to SU-8 and they can be bonded to Adhesive SU-8 on the coverplate.

3.3. Solid-phase extraction

SPE concentration was made with Isolute ENV+ SPE material. The SPE reservoir of the chip was easily filled with the wetted extraction matrix. Due to the very hydrophobic nature of ENV+, charged molecules will not be retained in SPE matrix [33]. The extraction efficiency of acids can be optimized by adjusting the pH of the sample solution at least two units lower than the pK_a of the analyte [34]. Due to the pK_a value 6.4 of fluorescein, the aqueous stock solution of 1 mg/ml fluorescein was diluted with 10 mM acetic acid (pH 3.4). This treatment ensured that fluorescein was uncharged and retained in the SPE matrix. Sample breakthrough was not observed due to fluorescein's high affinity for the ENV+ material.

The electrokinetic separation was started immediately after the elution buffer reached the SPE reservoir. Therefore the elution buffer had to conduct electricity and fluorescein had to be charged in this buffer. Five hundred micromolars CAPS (pH 10.4)–ethanol (40:60, v/v) met those criteria. When the elution buffer reached the SPE reservoir, the LIF signal increased sharply in SPE reservoir. The pumping of elution buffer was stopped, when the signal in SPE reservoir reached the plateau or the highest point. Fig. 8 shows the fluorescence detection of the SPE reservoir and separation channel at the same time.

3.4. Separation

Immediately after elution the sample was electrokinetically moved into the separation channel, which contained 120 mM CAPS, pH 10.1. The detection point was located at 24 mm from

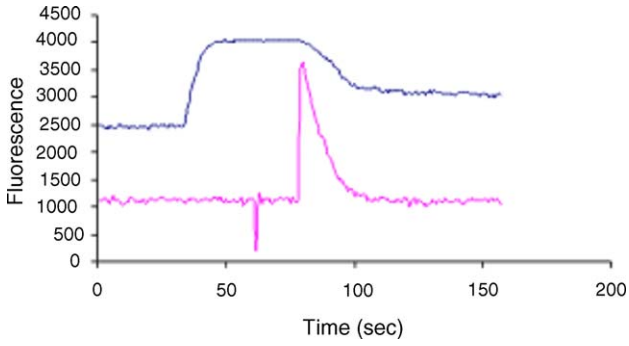

Fig. 8. The upper line shows the signal of the SPE reservoir. The signal increases sharply in 34 s, when the elution buffer reached the SPE reservoir. The pumping of the elution buffer was stopped approximately in 50 s, when the signal reached a plateau. During 50–70 s the elution buffer inlet and waste line were closed and the separation channel inlet and outlet were opened. The pumping of separation buffer with speed of 13.7 μl/min was started at the same time as the high voltage of 4 kV was turned on at 70 s. A decrease in the signal in the SPE reservoir indicates that analytes migrated into the separation channel. The signal did not decrease to the baseline due to incomplete elution. The lower line shows the signal of the separation channel. Approximately after 10 s the high voltage was turned on a peak of 26.6 μM fluorescein was observed at the detector.

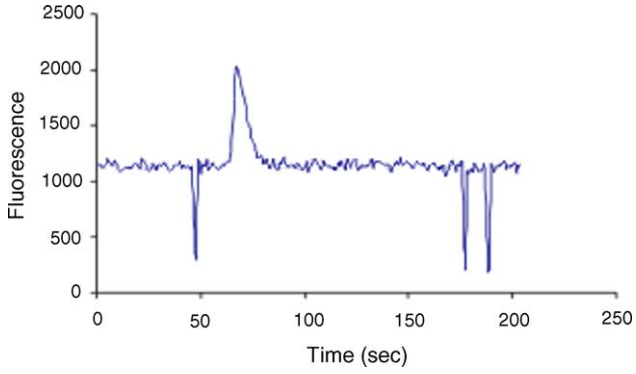

Fig. 9. Electropherogram of 2.66 μM fluorescein. Electrolyte solution: 120 mM CAPS (pH 10.1), elution buffer: 500 mM CAPS (pH 10.4)–ethanol (40:60, v/v), voltage 4 kV, pumping 13.7 μl/min. Approximately separation time 13 s. Effective separation length 24 mm.

the SPE reservoir. The fluorescein was successfully extracted from sample solution, injected into microchannel and detected. Fig. 9 shows the result for 2.66 μM fluorescein. The whole analysis – condition of the SPE matrix, sample loading, buffer wash, elution of analyte and separation – was carried out in less than 15 min. With one chip it was possible to make at least twenty analyses.

The SPE-ZE analyses showed that the procedure was reproducible. Relative standard deviation ($n = 4$) was calculated from the peak heights and areas for 26.6 μM fluorescein. The standard deviations of the peak heights were 17.9% and of the peak areas 19.7%. All the reproducibility measurements were made on a same chip.

4. Conclusions

Integrated SPE-ZE microfluidic chip has been designed and fabricated. Fabrication process has been optimized to produce high yield of large area SU-8 chips. Process innovations in

adhesive wafer bonding and in double coating-single exposure approach reduced alignment errors in fabrication of thick SU-8 structures. The process minimizes film stresses and greatly improves fabrication yield. Yield of functioning chips was 75% after process optimization. Fluidic and electrical behavior of the chip has been simulated. According to the simulations pillar-type bead filter shows uniform fluid flow which ensures that all the matrix in the SPE reservoir is available for the extraction. From the simulations it can also be noticed that electric field is uniform in the reservoir and therefore the electrokinetic transportation of the analyte from the reservoir to the electrophoresis channel occurs as desired. Fluidic tests with fluorescein samples showed successful extraction, elution and detection of the analyte on the SPE-ZE chip.

Acknowledgement

This work was financially supported by National Technology Agency of Finland (project no. 40339/02).

References

[1] S. Jacobson, C. Culbertson, J. Daler, M. Ramsey, Anal. Chem. 70 (1998) 3476.
[2] P. Kriikku, B. Grass, A. Hokkanen, I. Stuns, H. Siren, Electrophoresis 25 (2004) 1687.
[3] Y. Saito, K. Jinno, J. Chromatogr. A 1000 (2003) 53.
[4] Y. Saito, K. Jinno, T. Greibrokk, J. Sep. Sci. 27 (2004) 1379.
[5] N. Guzman, Electrophoresis 24 (2003) 3718.
[6] J. Kutter, S. Jacobson, M. Ramsey, J. Microcolumn Sep. 12 (2000) 93.
[7] K. Wolfe, M. Breadmore, J. Ferrance, M. Power, J. Conroy, P. Norris, J. Landers, Electrophoresis 23 (2002) 727.
[8] E. Verpoorte, Lab Chip 3 (2003) 60N.
[9] E. Oesterbroek, A. van den Berg (Eds.), Lab-on-Chip: Miniaturized Systems (Bio)Chemical Analysis and Synthesis, Elsevier, Amsterdam, 2003, p. 187.
[10] J. Choi, C. Ahn, S. Bhansali, T. Henderson, Sens. Actuators B 68 (2000) 34.
[11] A. Meng, A. Wang, R. White, Proceedings of Transducers 97, Sendai, Japan, The Institute of Electrical Engineers of Japan, Tokyo, Japan, 1997, pp. 876–879.
[12] G.-L. Lettieri, A. Dodge, G. Boer, N. de Rooij, E. Verpoorte, Lab Chip 3 (2003) 34.
[13] H. Andersson, C. Jönsson, C. Moberg, G. Stemme, Electrophoresis 22 (2001) 3876.
[14] H. Andersson, W. van der Wijngaart, P. Enokson, G. Stemme, Sens. Actuators B 67 (2000) 203.
[15] R. Oleschuk, L. Shultz-Lockyear, Y. Ning, J. Harrison, Anal. Chem. 73 (2000) 585.
[16] K. Mogensen, N. Petersen, J. Hübner, J. Kutter, Electrophoresis 22 (2001) 3930.
[17] T. Ujiie, T. Kikuchi, T. Ichiki, Y. Horiike, Jpn. J. Appl. Phys. 39 (2000) 3677.
[18] J. Shaw, J. Gelorme, N. LaBianca, W. Conley, S. Holmes, IBM J. Res. Dev. 41 (1997) 81.
[19] K. Lee, N. LaBianca, S. Rishton, S. Zohlgharnain, J. Gelorme, J. Shaw, H.-P. Chang, J. Vac. Sci. Technol. B 13 (1995) 3012.
[20] H. Lorenz, M. Despont, M. Fahrni, N. LaBianca, P. Vettiger, P. Renaud, J. Micromech. Microeng. 7 (1997) 121.
[21] H. Lorenz, M. Despont, P. Vettiger, P. Renaud, Microsyst. Technol. 4 (1998) 143.
[22] P. Dentinger, K. Krafcik, K. Simison, R. Janek, J. Hachman, Microelectron. Eng. 61/62 (2002) 1001.
[23] R. Jackman, T. Floyd, R. Ghodssi, M. Schmidt, K. Jensen, J. Micromech. Microeng. 11 (2001) 263.
[24] S. Tuomikoski, T. Sikanen, R. Kostiainen, T. Kotiaho, S. Franssila, Proceedings of MICROTAS 2004, Malmö, Sweden, Royal Society of Chemistry, Cambridge, UK, 2004, pp. 339–341.
[25] D. Duffy, C. McDonald, O. Schueller, G. Whitesides, Anal. Chem. 70 (1998) 4974.
[26] K. Huikko, P. Östman, K. Grigoras, S. Tuomikoski, V.-M. Tiainen, A. Soininen, K. Puolanne, A. Manz, S. Franssila, R. Kostiainen, T. Kotiaho, Lab Chip 3 (2003) 67.
[27] M. Heuschkel, L. Guérin, B. Buisson, D. Bertrand, P. Renaud, Sens. Actuators B 48 (1998) 356.
[28] L. Guerin, M. Bossel, M. Demierre, S. Calmes, P. Renaud, Proceedings of Transducers 97, Sendai, Japan, Institute of Electrical Engineers of Japan, Tokyo, Japan, 1997, pp. 1419–1422.
[29] P. Renaud, H. van Lintel, M. Heuschkel, L. Guerin, Proceedings of the MICROTAS 1998, Banff Canada, Kluwer, Dordrecht, 1998, pp. 17–22.
[30] S. Tuomikoski, S. Franssila, Sens. Actuators A 120 (2005) 408.
[31] S. Tuomikoski, S. Franssila, Phys. Scripta T114 (2004) 223.
[32] H. Lorenz, M. Laudon, P. Renaud, Microelectron. Eng. 41/42 (1998) 371.
[33] C. Franke, H. Westerholm, R. Niessner, Water Res. 31 (1997) 2633.
[34] Technical Note 109, Argonaut Technologies, 2004.